Zirconia powders obtained from zirconyl nitrate by precipitation with the varied concentration of the ammonium hydroxide

Tatiana E. Lomakina[1,*], Yaroslav V. Konakov[1], Ivan Yu. Archakov[1], Olga Yu. Kurapova[2], Vladimir G. Konakov[1]

[1]*Institute for Problems of Mechanical Engineering V.O., Bolshoj pr., 61, St. Petersburg 199178, Russia*

[2]*Elcogen Oy, Niittyvillankuja 4, 01510 Vantaa, Finland*

Received 23 October 2025; received in revised form 6 December 2025; accepted 23 January 2026

Abstract

Phase stability and degradation of zirconia-based ceramics, which represents a very important industrial material, highly depend on the dispersity and structure of the raw powder materials. The aim of this research was to study the influence of the concentration of the precipitating agent (ammonia) on the agglomeration, morphology and crystallisation of zirconia particles during precipitation from zirconyl nitrate salt. By potentiometric titration, it was shown that precipitation with 1 M ammonia solution balances the processes of hydrolysis and precipitation. According to STA, XRD and PSD data crystallisation temperature decreases by 77 °C when ammonia concentration is reduced from 0.5 to 0.2 M resulting in the kinetic stabilisation of the tetragonal zirconia at 550 °C. BET data showed that the highest specific surface area of the powders was obtained in the case of precipitation from 0.5 and 1 M ammonium hydroxide solutions.

Keywords*: zirconia; co-precipitation; nanoparticles; phase transition; precipitator*

I. Introduction

The unique set of characteristics makes stabilised zirconia ceramics one of the most sought-after oxide materials in the modern industry [1,2]. Indeed, tetragonal zirconia possessing biocompatibility, outstanding bending strength (900–1200 MPa), and fracture toughness of 5–10 MPa·m$^{1/2}$ [2–5] provides the wide use of zirconia-based ceramics as one of the basic materials in dentistry, joint surgery and orthopaedy. The combination of high temperature stability with the oxygen conductivity of cubic zirconia promotes the wide use of such ceramics as an electrolyte in the solid oxide fuel cells [6–8], gas controlling sensors in metallurgy, glass-making and other high temperature technologies [9–11]. High mechanical characteristics coupled with chemical resistivity at high temperatures stipulate the use of zirconia ceramics in aviation and space technologies as a promising construction material where ZrO_2-based materials are used as thermal barriers coatings [12,13].

The industrial need for prolonging the lifetime and increasing performance of the stabilised zirconia ceramics for each of the applications sets the general requirements on the raw materials and precursor powders. Independently of the applications, these powders should be chemically pure and possess a desired dispersity [8,14]. In addition, phase stability of the powders is a key point here since the degradation of partially and fully stabilised zirconia is well known phenomena limiting the lifetime of ceramics [15,16]. Elimination of the monoclinic phase formation in such ceramics is possible when wet chemistry synthesis approaches are used for the precursor powders preparation [17–19]. Indeed, many industrial manufacturers of zirconia powders are using the precipitation techniques providing a set of variable parameters for better control of the precursor powder dispersity [20,21].

The state-of-the-art results devoted to the chemical wet processing of zirconia can be found in numerous papers [22–24]. Precipitation parameters such as pH, temperature, reagents concentration, nature of salts and precipitator affect the final precursor powders properties [22,25]. Most of them were addressed for the case of precipitation using zirconyl chloride [20,21,23]. It was already shown [20] that powders dispersity and phase formation of zirconia precipitated by ammonia from zirconyl chloride solutions of different concentrations and pH varied significantly. The sample produced at pH=12

*Corresponding author: tel: +7 93 13732960
e-mail: *lomakina.te@edu.spbstu.ru*

and a concentration of zirconyl nitrate of 0.81 M resulted in approximately 49 nm particles, being significantly smaller than those produced under the other studied conditions [20]. Further calcination resulted in the larger amount of tetragonal zirconia in the obtained powder. Similar results were obtained by Lomakina *et al*. [26] when the effect of the zirconia salt nature (zirconyl nitrate and chloride) on the final precursor powders properties (powders dispersity and phase composition) was investigated. The differences in the hydrolysis and precipitation behaviour of two zirconyl salts were discussed as well as their effect on the crystallisation temperatures and enthalpies. Keenan [27] reported the increase in the specific surface area of the zirconia precursor powders calcined at 500 °C with the increase in the ammonia precipitator contents. The decrease in the median crystallite size from 105 to 10 nm was observed.

Huang *et al.* [28] used different precipitants (ammonium hydroxide, ammonium bicarbonate, oxalic acid and urea) to study the effect of precipitants on the phase composition, stoichiometry and particle sizes of yttria-stabilised zirconia powders. The crystallisation temperature of the cubic zirconia solid solution was the lowest (about 400 °C) when ammonia was used as a precipitant, while it was about 500 °C in the case of other three types of precipitants (ammonium bicarbonate, oxalic acid and urea) that were used. Ammonium bicarbonate was shown to be unable to precipitate ZrO^{2+} effectively in the solution, resulting in the formation of the cubic $Y_{0.18}Zr_{0.82}O_{1.91}$ compound at 1000 °C. Urea was suggested as an optimal precipitating agent despite the challenges associated with the co-precipitation process.

Vörös-Horváth *et al*. [29] considered the use of ammonia to be a key parameter for monodispersed SiO_2 spherical particles production. The ammonia effect on the sol particles can be compared to the alkali effect [30]. Indeed, alkalis are rather strong electrolytes; their effect on the sol particles could be explained using the double layer theory (DLVO). According to this theory, the electrolyte ions affect the colloidal characteristics of the suspension, i.e. the width of the electrical double layer diffuse part determining the possibility of their effective collision with following agglomeration. The higher the ionic strength of the solution, the lower the energetic barrier; hence, the possibility of particles agglomeration in sol is high. The use of ammonia as a weak and low dissociating base (α < 30%) gives an opportunity to provide the enough amounts of OH^- ions at a low ionic strength of the solution. In addition, the use of ammonia results in the absence of the contaminating precipitator residuals in the following synthesis steps – washing, drying and annealing. Kim *et al.* [31] compared the effect of 0.6 M ammonia contents on the SiO_2, TiO_2 and ZrO_2 nanoparticles synthesis using the sol-gel approach: the size of silica particles gradually increased to about 150 nm, while the final sizes (92 and 42 nm) of ZrO_2 and TiO_2 particles became significantly smaller than that of SiO_2; more intensive hydrolysis of the initial metal salts was pointed out for TiO_2 and ZrO_2 fabrication.

To sum up, it has been observed that the literature data on the precipitation is rather contradictory. Thus, the task of the present work was the systematic study of the ammonia contents effect on the hydrolysis and precipitation processes of the zirconyl nitrate salts, resulted precursor powders dispersity and determination of the optimal precipitator contents for the process. As shown in our recent work [26], the use of nitrate is beneficial compared to the chloride as zirconyl nitrate precipitation is accompanied by the stepwise and intensive hydrolysis, whereas the simultaneous hydrolysis and precipitation take place in the zirconyl chloride case in all titration range. The present study contributes to a better understanding of the relationship between synthesis conditions and the resulting precursor powder characteristics, paving the way for improved zirconia production methods at the laboratory and industrial scale.

II. Experimental

2.1. Sample preparation

Undoped ZrO_2 and tetragonal 4 mol% ytrria-stabilised zirconia (4YSZ) samples were synthesized using the following reagents: $ZrO(NO_3)_2{\cdot}6H_2O$ (CAS 14985-18-3, Acros Organics, Belgium, 99.5%), $Y(NO_3)_3{\cdot}6H_2O$ (CAS 13494-98-9, Acros Organics, Belgium, 99.9%), aqueous ammonia solution (CAS 1336-21-6, Vecton, Russia) and distilled water. The reverse co-precipitation approach followed by freezing of the resulting gel in the liquid nitrogen was used [23,26] to produce the precursor powders. In the first step, 0.1 M aqueous salt solutions were prepared by dissolving the nitrate hydrates in water and thoroughly mixing. Then, the solutions were added drop-wise at a rate of ~1–2 ml/min into the ammonia aqueous solution of the varied concentration (0.2–5.0 M). Co-precipitation was performed in an ice bath in the temperature range 0–5 °C with a permanent mixing, which resulted in the formation of hydroxide mixtures. The produced gels were aged for 48 h, filtered through the Büchner funnel with an ashless paper filter (Grade 589/3 blue ribbon filter, an average pore size of ~ 2 μm) to remove the residual mother solution, and washed by the distilled water to the neutral pH level. Then the gels were subjected to freeze-drying in liquid nitrogen (the details are given in Ref. [32]) and finally the obtained powders were annealed at 550 and 800 °C for 2 h in air.

The following samples were produced: i) undoped zirconia samples $T_{0.2}$, $T_{0.5}$, T_1, T_3 and T_5 synthesised

using 0.2, 0.5, 1.0, 3.0 and 5.0 M ammonia solutions, respectively, and ii) T-YSZ41 (the reference 4YSZ sample) synthesised using 1.0 M ammonia solution.

2.2. Characterisation methods

Potentiometric titration (Ion-meter IS-120, Russia, with a glass electrode as an indication electrode and saturated silver chloride electrode (Ag/AgCl, Cl^-) as a reference electrode) was used to study the precipitation processes and 20 ml aliquot was taken for each titration. Simultaneous thermal analysis (STA, NETZSCH-STA 449F1 Jupiter, Germany) was used to characterize the thermal effects during the synthesis (heating rate 10 °C/min, 40 to 1100 °C, N_2 flow). Particle size distribution (PSD) analysis was carried our using Horiba Partica LA-950, Japan. The specific surface area was investigated by the nitrogen sorption/desorption using Nova 1200e (Quantachrome Instruments, USA) surface area and micropore size analyser. The phase identification was performed by X-ray diffraction analysis (XRD, Shimadzu XRD-6000, Japan) using Cu-Kα radiation at λ = 1.5406 Å, accelerating voltage of 40 kV at 30 mA current from 5 to 80° with 0.02° resolution and 1 °C/min scanning speed. Phase identification was carried our using PDF-2 database (released 2021). Crystallite sizes were estimated using Sherrer's formula:

$$D_{XRD} = \frac{k \cdot \lambda}{\beta \cdot \cos\theta} \quad (1)$$

where D_{XRD} is a mean crystallite/particle size, k is Scherrer constant being the shape factor (typically taken as k = 1), λ is X-ray wavelength (λ = 1.5406 Å), β is full width at half maximum (FWHM) of the diffraction peak and θ is Bragg diffraction angle. Crystallinity, K, was calculated using the software of the diffractometer as the ratio of crystalline to amorphous phases. Scanning electron microscopy (SEM, Zeiss Auriga Crossbeam, Germany; accelerating voltage 30 kV) was used to analyse the morphology of the powders. The samples were fixed onto the carbon scotch tape and no conducting coating was applied. Materials, synthesis procedure and characterisation of the samples were described in more detail in our previous work [26].

III. Results and discussion

3.1. The effect of ammonia concentration

Potentiometric titration provides information on the processes of hydrolysis and precipitation in the zirconia solution upon ammonia addition. Since the change in the ammonia concentration may change the sequence of hydrolysis and precipitation steps, titrations of zirconyl nitrate with 0.2–5 M ammonia solutions were performed. The results are presented in Fig. 1.

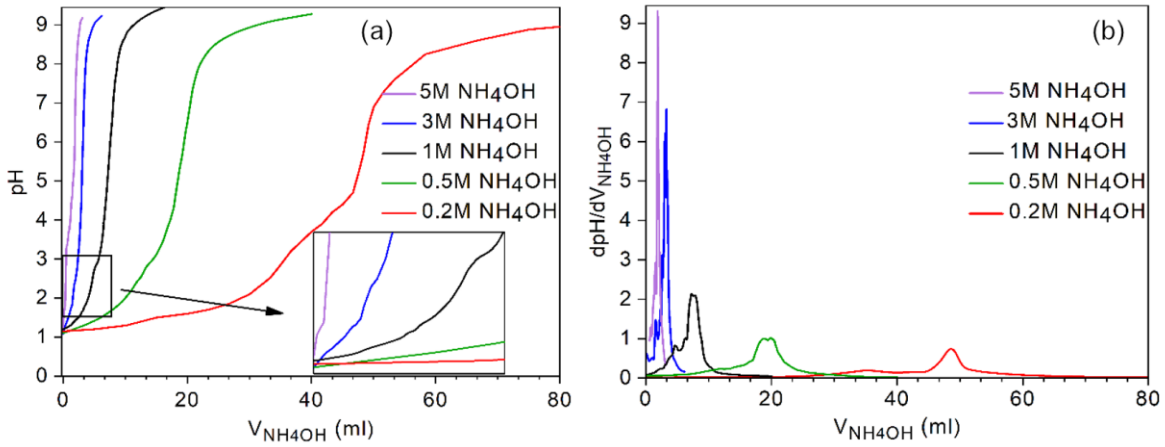

Figure 1. NH_4OH titration curves of initial 0.1M $ZrO(NO_3)_2$ aqueous solutions (a) and the first derivatives of the obtained titration curves (b). Insert in Fig. 1a is the magnified region of the inflection points corresponding to the hydrolysis process

Titration curves obtained for all investigated NH_4OH concentrations are similar (Fig. 1). The initial zirconyl nitrate solution has an acidic media reaction (pH ~1.2). It is due to almost full hydrolysis of ZrO^{2+} to $ZrO(OH)^+$ in the first hydrolysis stage. The initial region of the titration curves (pH from 1.2 to 1.6) is characterized by neutralisation of the $ZrO(OH)^+$ ions of basic zirconyl by 60.2% and simultaneous hydrolysis at the first stage. The neutralisation degree was estimated based on the concentration of protons in the initial solution and the solution after the titration. The depth of hydrolysis was calculated to be 25%. It is based on the initial pH value and the amount of ammonium hydroxide needed for the neutralisation of the protons neutralised in the equivalence point and those that elaborated during the hydrolysis step. Nearly 25% of the final $ZrO(OH)_2$ amount is formed here. The value obtained indicates that the tetramers of

basic zirconyl in the solutions are ready for the polymerisation process [26]. Since the precipitation rate significantly depends on the ammonia concentration, the titration curves are expected to be different from each other with the further pH increase.

The region of the titration curves corresponding to pH from 1.6 to ~4 is the most important as it is referred to the competition between the hydrolysis and precipitation [26]. As seen from Fig. 1, the inflection points on the titration curves obtained using 0.2 and 0.5 M ammonia are located at pH 1.66 and 2.00. In these two cases, the values of the inflection points are below 2.25 giving the evidence of the ammonia deficiency when low concentrations of ammonia are used. It results in the domination of hydrolysis over the precipitation. Latter limits the dendritic polymeric chains formation in zirconia hydroxide and results in their lamellar growth. Such variation of the precipitation favours fine nanoparticles formation; however, it hinders the formation of a three-dimensional special network of $[Zr(OH)_4]_n$ gel. In addition, it often results in the lower surface area of the powder. An increase in the ammonia concentration to 1 M results in the shifting of the inflection point to pH 2.24. Here the precipitation starts prevailing over the hydrolysis. At pH of 2.24 the depth of hydrolysis in the second stage is 50%. The obtained value shows that the clusters of the basic zirconyl are turned to oligomers and start precipitation into the polymeric gel [26]. Note that tetramer clusters are absent in the reaction media.

Further increase in the precipitator concentration results in the inflection point shift to 2.3 and 2.72 for titration curves obtained using 3 and 5 M ammonia, respectively. The precipitation rate here is too high and the process is uncontrolled. The agglomeration of the precursor powder can be expected. It may likely result in decreased specific surface area and spongy powder structure having large interparticle pores. Overall comparison of the inflection points positions on the titration curves shows that when the titration is performed using ammonia with the concentration of 1 M or higher, precipitation prevails over the hydrolysis, whereas the use of low ammonia concentrations results in the hydrolysis being the primary process in the solution.

The region of the curve from pH 4 to 7 refers to the amount of ammonia needed to neutralise all the protons in the solution, i.e. the equivalence point. From the positions of the equivalence points, i.e. 0.20, 0.21, 0.16, 0.21 and 0.20 for 0.2, 0.5, 1, 3 and 5 M ammonia, it is seen that in the case of 1 M ammonia concentration the obtained value is the closest to the initial concentration of zirconyl nitrate in the solution. The determined deviation in the concentration obtained for both diluted ammonia and the concentrated one is the same. This leads to the conclusion that the reason for over-titration is the ageing of the gel and the acidification of the solution due to the oxolation process. This process accounts for the association of $ZrO(OH)^+$ particles into Zr–O–Zr and free protons. Thus, synthesising the gel by precipitation with a 1 M ammonia solution balances the processes of hydrolysis and precipitation. In this case 0.1 M $ZrO(NO_3)_2$ solution is evenly distributed in a sufficient amount of precipitant, and excess of any reagent is avoided.

3.2. Structure and thermal effects upon heating

Thermal analysis was used to clarify the effect of ammonia concentration on the processes of dehydration and crystallization in the xerogels of the undoped zirconia (Fig. 2). Figure 2a demonstrates the differential scanning calorimetry (DSC) curves and information on temperatures and thermal effects corresponding to these processes in ZrO_2 powders, while Fig. 2b shows thermogravimetry data (TG curve), that gives an opportunity to evaluate the mass losses in the xerogel matrices during the heating.

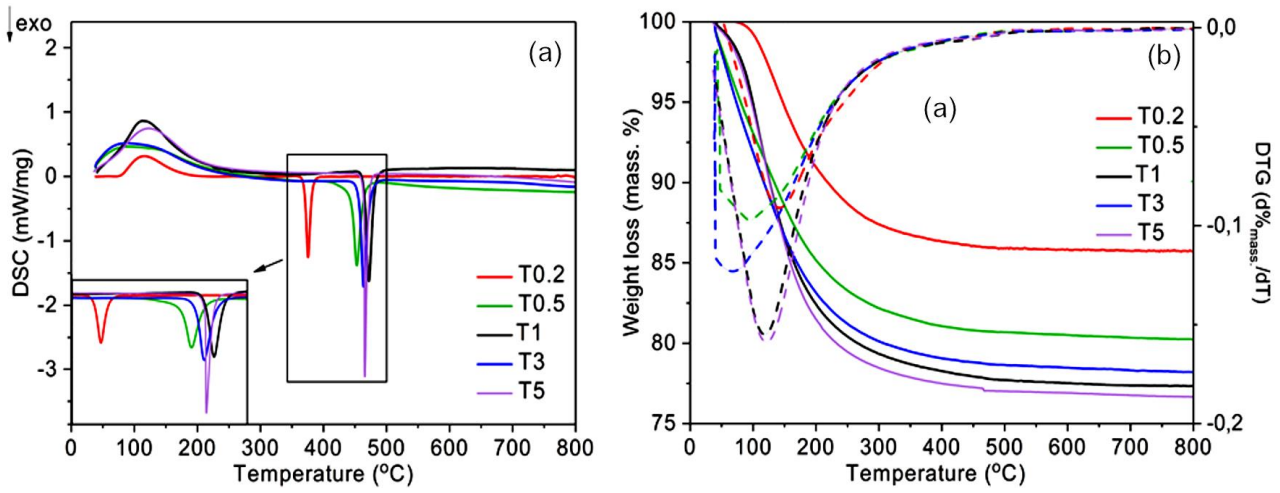

Figure 2. Differential scanning calorimetry (DSC) curves (a) and thermogravimetry curves (b) of T0.2–T5 precursor powders. Insert in Fig. 2a is the magnified region of the peaks corresponding to the crystallization process

All DSC curves in Fig. 2a demonstrate the prolonged endothermic effect with the maxima in the temperature range of 105–140 °C. According to Fig. 2b, they are characterized by significant weight losses and could be attributed to the dehydration process. Considering the extended shape of the peaks typical for all samples studied, one can conclude that the processes of the adsorbed and structural water removal proceeded simultaneously up to 300 °C (the rate of this removal was rather low). More detailed results on the thermal effects, temperatures and calculated values for the dehydration/crystallization enthalpies and weight losses are listed in Table 1 together with the data for the reference sample of tetragonal zirconia T-YSZ41.

As it can be seen from the calculated data in Table 1, the overall weight losses increase with the ammonia contents increase. Generally, the values of dehydration enthalpy show the same trend except for the value for the T_1 sample. Generally, the losses of the structurally bonded water could be evaluated within the assumption that all such water is present in the form of OH^- (i.e. hydroxides $Zr(OH)_4$ and $Y(OH)_3$). The weight loss values of 22.1 and 21.9 wt.% for the undoped ZrO_2 and 4YSZ samples, respectively, were obtained as a result of such evaluation. Comparing these results with the data from Table 1, one can conclude that the weight losses registered for the $T_{0.5}$, T_1, T_3 and T_5 samples could be attributed to the structural-bonded water losses. Similar to the behaviour of the silicon hydroxide reported in the literature [33], the relatively small weight losses registered for the $T_{0.2}$ sample might be due to hydroxide particles not being completely hydrated at low precipitator concentration. However, these particles are also included in the precipitation process. It results in accelerated gel ageing (oxolation) and the bonded water is lost already at the synthesis step. Thus, the significant part of the bonded water is not retained in the $T_{0.2}$ powder. The discussed results are consistent with the titration data above. However, weight losses registered for the stabilised zirconia exceeded the above estimates. Possibly, it is due to a relatively high amount of the physically adsorbed water.

Table 1. Dehydration/crystallization temperatures and enthalpies as well as weight losses of the prepared samples

Specimen	Dehydration temperature [°C]	Dehydration enthalpy [kJ/mol]	Crystallization temperature [°C]	Crystallization enthalpy [kJ/mol]	Overall weight loss [%]
$T_{0.2}$	127±1	14±1	375±1	-8±1	13.7±0.1
$T_{0.5}$	107±1	31±3	452±1	-14±1	19.0±0.1
T_1	117±1	48±5	472±1	-14±1	22.1±0.1
T_3	107±1	33±3	464±1	-15±1	20.9±0.1
T_5	125±1	44±4	463±1	-11±1	22.5±0.1
T-YSZ41	138±1	90±9	517±1	-15±1	25.9±0.1

The exothermal processes typical for all studied samples were registered in the undoped zirconia in the temperature range from 375 to 472 °C. They can be attributed to the amorphous-to-crystal phase transition. As it can be seen from Fig. 3 and Table 1, the crystallisation temperature of the $T_{0.2}$ sample obtained using 0.2 M ammonia as a precipitating agent is 77 °C lower compared to the T_5 sample, i.e. 375±1 °C vs. 452±1 °C. Further increase in the ammonia concentration does not induce the significant change in the crystallisation temperature.

As it was discussed earlier [26], the deposition rate during the ammonia-catalysed condensation increases with the ammonia contents. Hence one can assume that the close values of the crystallization temperatures typical for the $T_{0.5}$, T_1, T_3 and T_5 samples are due to the fact that the median particle sizes here overreached some critical value stimulating the accelerated formation of the tetragonal zirconia, as discussed in the literature [34,35]. Such a decrease of the crystallization temperature can be due to the higher dispersity or different morphology of the xerogel. To confirm this hypothesis, the morphologies of the powders were analysed by SEM under different resolution. The results are presented in Fig. 4.

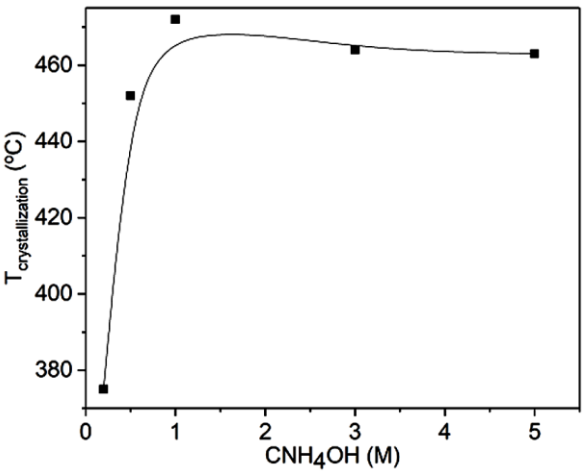

Figure 3. The dependence of the crystallization temperature on the concentration of ammonium hydroxide

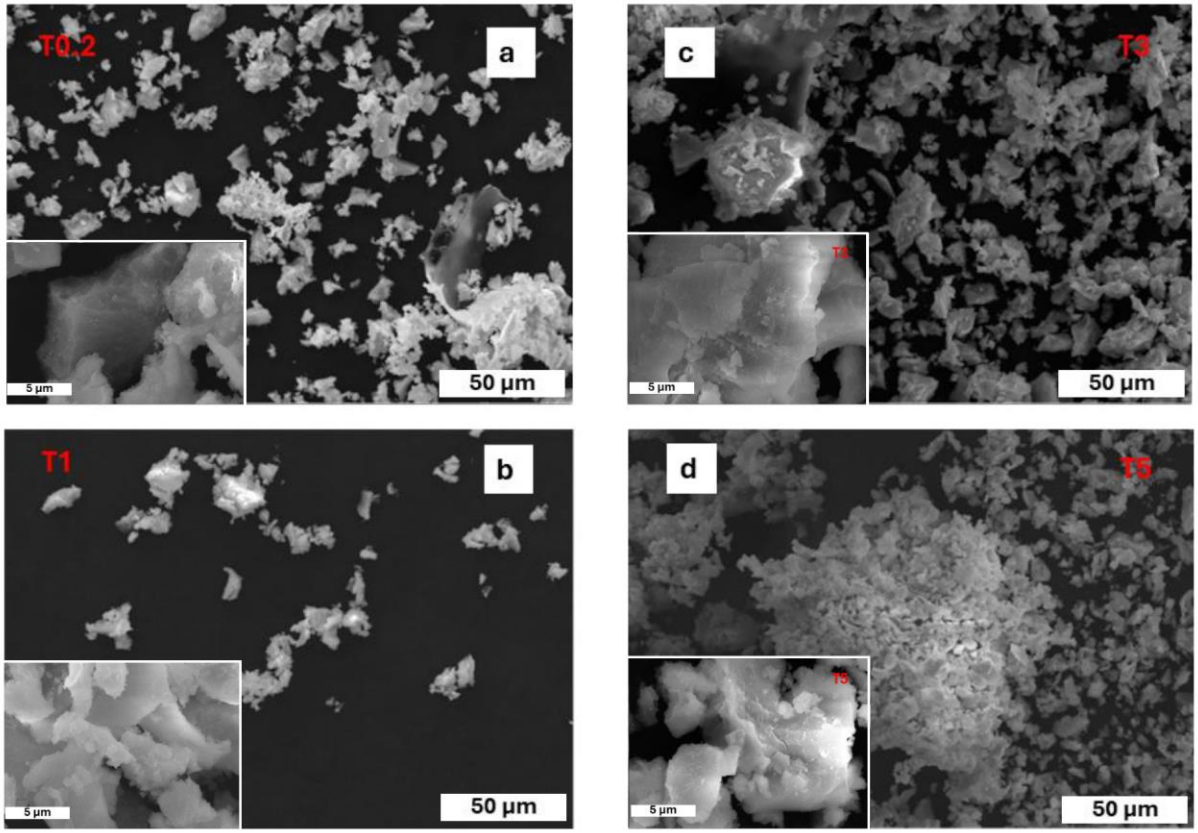

Figure 4. SEM images of: a) $T_{0.2}$, b) T_1 c) T_3 and d) T_5 samples

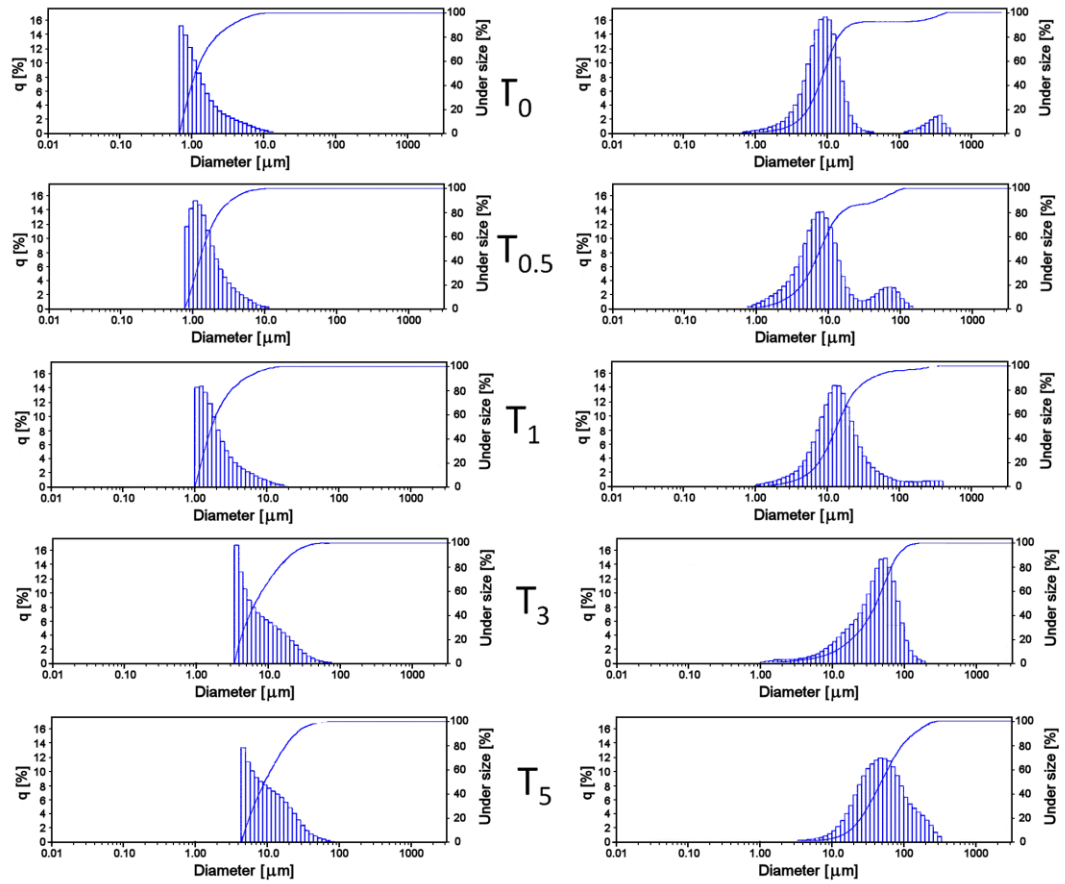

Figure 5. The comparison of the PSD analysis results, left column shows distribution by numbers and right column by volume

As it can be seen from Fig. 4, all samples are composed of the dendrite agglomerates having irregular shapes. Such a shape is typical for zirconia-based samples [26]. The sample T_5 is characterized by the highest degree of agglomeration whereas the samples T_1 has the lowest, being in accordance with the potentiometric titration analysis. The increase of ammonia concentration up to 3–5 M results in the formation of large aggregates with the shape close to spherical. The sample $T_{0.2}$ contains a mixture dendrites and lamellar particles (Fig. 4a). The formation of the particles with lamellar morphology most likely is a result of the hydrolysed zirconia in the precipitate. Indeed, according to the titration data, the domination of the hydrolysis processes over the precipitation limits the growth of the dendrite polymeric chains and favours the formation of the lamellar structure [33]. Under higher magnification (insets in Fig. 4) it is seen that the agglomerates in the samples $T_{0.2}$–T_5 are rather dense and composed of submicron particles. Overall, their morphologies are similar, however a sharp edge of the lamellar particle is seen in the sample $T_{0.2}$.

As for the stabilised zirconia sample T-YSZ41, the crystallization temperature of 517±1 °C is higher than that for the undoped samples. This effect is the consequence of the material characteristics change due to the zirconia solid solution formation. The precipitator concentration also affects the crystallization enthalpy values. As seen from Fig. 2a and Table 1, the amorphous-to-crystal phase transition enthalpies for the $T_{0.5}$, T_1, T_3 and T-YSZ41 samples agree well with the reference value of -15±1 kJ/mol [36] while the results obtained for both minimal ($T_{0.2}$) and maximal (T_5) ammonia concentrations are significantly lower.

Table 2. Median particle size, specific surface area and the residual weight (%) of the powders

Specimen	Median particle size, [μm]	Specific surface area, [m^2/g]	Residual weight [%]
$T_{0.2}$	1.13±0.01	171±2	86.3±0.1
$T_{0.5}$	1.38±0.01	199±2	81.0±0.1
T_1	1.72±0.01	197±2	77.9±0.1
T_3	6.69±0.01	147±1	79.1±0.1
T_5	9.44±0.01	152±2	77.5±0.1
T-YSZ41	0.92±0.01	207±2	74.1±0.1

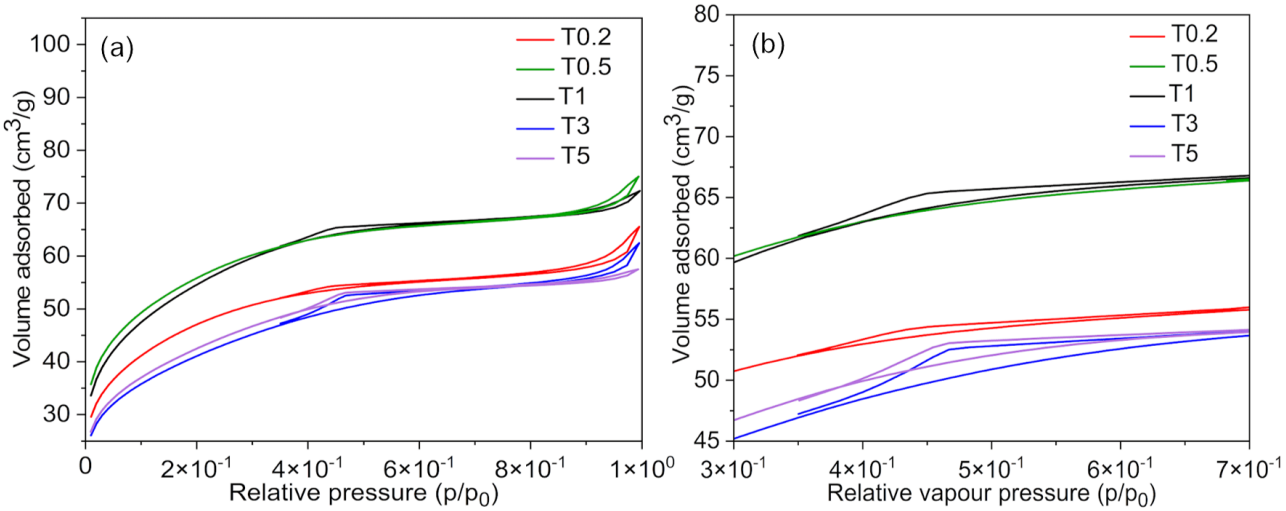

Figure 6. Sorption/desorption curves for the samples: a) adsorption isotherms and b) the magnified region of the isotherm corresponding to the hysteresis loop

Figure 5 compares particle size distributions obtained for the samples $T_{0.2}$–T_5. Median particle sizes for these powders are listed in Table 2. Note that the ultrasound was applied to all studied samples to break the agglomerates. As seen from the presented data, synthesis with lower ammonia contents ($T_{0.2}$, $T_{0.5}$ and T_1 samples) provides rather similar particle distributions with close median sizes and bimodal shapes of volume distributions. However, some slight increase in the median particle size is evident: the lower precipitator contents give an opportunity to obtain particles with dimensions below 1 μm, while the increase in the ammonia contents provides particles with the typical dimensions higher than 1 μm. As for the distribution by volume, an increase in the ammonia contents provides almost complete decrease in the second peak intensity. The $T_{0.2}$ sample has a significant volume fraction of large agglomerates of 300–500 μm, originating from admixture of flakes seen in Fig. 4a. The maximum of the second peak

moves to 70–100 μm region in the case of the $T_{0.5}$ sample, while no bimodal distribution could be observed for the T_1 sample. This leads to the conclusion that morphology of the agglomerates is fully dendritic for the T_1 sample. Further increase in the precipitator contents gives rise to the significant increase in the median particle sizes from 1.1–1.7 to 6.7 and even 9.4 μm being in accordance with SEM results (see Fig. 4). In the same time, the number of large agglomerates with the dimensions close to 100 μm seems to be negligible, as seen in distributions by volume (Fig. 5). Hence, one can conclude that precipitation at low ammonia contents produces the major fraction of powder with rather small agglomerate sizes (median sizes ~1–1.5 μm) coupled with some amount of fairly large ones. The increase in the precipitator contents leads to an increase in the median particle size; the number of large agglomerates related to flakes formation is negligible here.

The specific surface area is one of the characteristics, also dependent on the synthesis conditions, in our case, on the precipitator (ammonia) contents. The results of BET analysis are shown in Fig. 6. As presented, adsorption/desorption curves for all samples correspond to the IV type of the adsorption isotherm indicating the presence of capillaries in the xerogel structure. Generally, such type of curve is typical for hydrated zirconia due to the presence of rather small pores in the powder particles [37]. The conclusion is consistent with the morphologies of samples presented in Fig. 4. The porosity likely originates from the space left between closely packed particles.

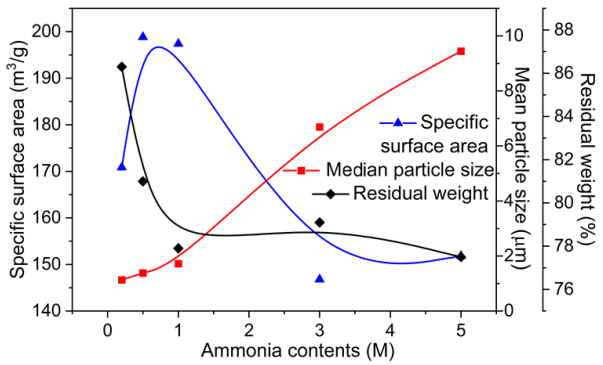

Figure 7. The effect of the precipitator contents on the specific surface area, median particle size and residual weight of the samples according to TG data

Let us discuss the ammonia content effect on the shape of the hysteresis of the adsorption isotherms. As seen from Fig. 6, the area of the hysteresis loop slightly increases as the precipitator content increases from 0.2 to 3 M (the samples $T_{0.2}$-T_3), and then it decreases when the concentration of the precipitator reaches 5 M (Fig. 6b). This fact supports the assumption that the lower packing density of the particles is due to the fast and non-controlled precipitation. In turn, it provides an increase in the agglomeration rate. As seen in Fig. 7, the dependence of specific surface area on the ammonia concentration has a maximum of 199±2 m^2/g in the range 0.5–1 M ammonia (Table 2). Overall, the obtained values are consistent with the literature data [26,37,38]. Remarkably, when the diluted ammonia solution of 0.2 M is used for zirconia precipitation, the specific surface area of the $T_{0.2}$ sample remains lower than the value for the $T_{0.5}$ sample (171±2 m^2/g). It is likely due to the bimodal distribution of the particles in the $T_{0.2}$ powder (Fig. 5) and a presence of the agglomerated particles. Lower surface area of the $T_{0.2}$ sample could be also due to the observed deviations from the typical xerogel structure resulting from the preferential formation of the spherical particles and lamellar particles [39]. Latter results in the additional compaction of the structure. The increase in the precipitator contents provides an increase in the particle sizes. Their agglomeration gives rise to the significant decrease in the specific surface area (the red curve in Fig. 7 and the data on the particle size in Table 2). Probably, the formation of large-sized pores or even a spongy-like structure is possible here [37].

In addition, the samples were annealed at the temperatures higher than phase transition temperature, i.e. at 550 and 800 °C for 2 h to obtain the information on the effect of ammonia concentration on the tetragonal phase stabilisation. The results are presented in Fig. 8 and Table 3 summarises quantitative data on the phase composition, crystallinity of the samples and compares crystallite sizes to median particle sizes.

As it can be seen from Fig. 8a, annealing at 550 °C for 2 h results in the formation of metastable tetragonal zirconia modification, being in accordance with the crystallization enthalpy data (Table 1). The precipitation by 0.2 M ammonia results in a pure tetragonal phase with the crystallinity, *K* of 49% and D_{xrd} of 79 nm. The increase in ammonia concentration to 0.5 and 1 M induces the small admixture of monoclinic phase, 8 and 9 wt.% for the $T_{0.5}$ and T_1 samples, respectively, followed by the slight increase of crystallinity for the sample $T_{0.5}$ to 52%. Further increase in the ammonia concentration results in the increased amount of monoclinic phase in the T_3 samples (13 wt.%, see Table 1), whereas the sample T_5 contains only 5 wt.% of monoclinic phase. Both samples are characterized by the lowest crystallinity, i.e. 45 and 44% for the T_3 and T_5 samples, respectively. Lower monoclinic content in the T_5 sample coupled with lower crystallinity and the largest agglomerate sizes indicates that 2 h of annealing at 550 °C is not enough to finish the crystallization process in the bulk of the agglomerate. The increase in the annealing temperature to 800 °C confirms this assumption and the amount of monoclinic phase in the

T_5 sample increases to nearly 53 % (Table 3). The sample $T_{0.2}$ shows remarkable stability of metastable tetragonal phase. The amount of monoclinic phase induced in the sample is only 9 wt.%. The sample T_1 stands out from the trend, resulting in the decreased amount of tetragonal phase. Table 3 reflects the relation between the crystallization process and changes in crystallite sizes. Crystallite sizes decrease for the samples characterized by a significant increase in the monoclinic phase content, indicating recrystallization. For the samples having low monoclinic phase content, the size of crystallites increases indicating the kinetic stabilisation of the tetragonal please. For all calcined samples (Table 3), the average particle size decreases significantly at 550 °C and becomes submicron, due to simultaneous crystallization and dehydration processes. As the temperature increases, the average particle size decreases or remains unchanged.

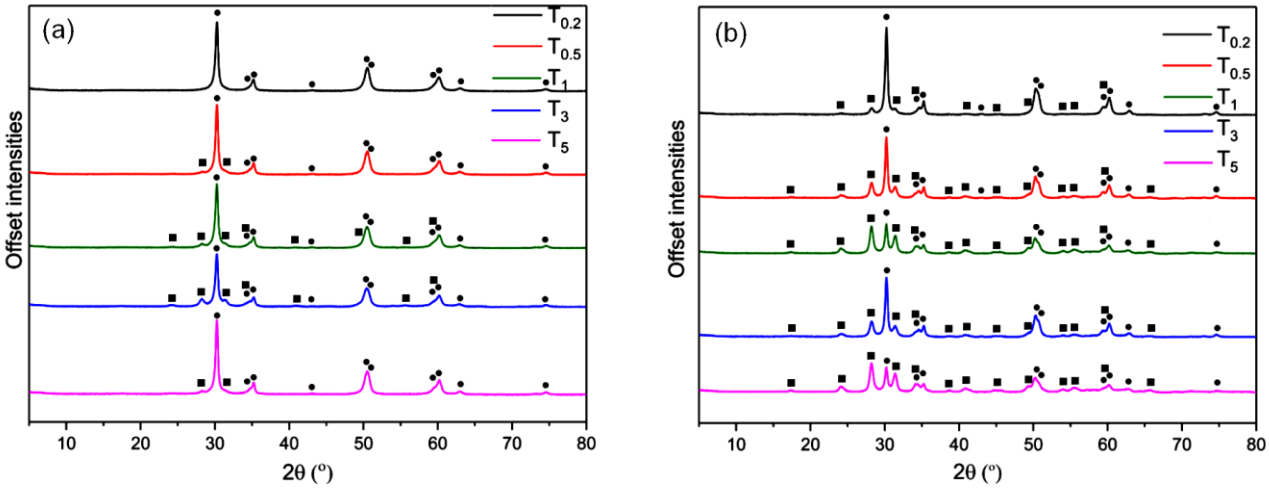

Figure 8. XRD patterns obtained for samples annealed at 550 °C (a) and at 800 °C (b) for 2 h; ■ denotes the monoclinic phase and ● – to the tetragonal one

Table 3. Phase composition, crystallinity, crystallite sizes based on XRD data and median particle sizes based on PSD data. P1 – monoclinic phase, P2 – tetragonal phase, 2θ = 30.20°, λ = 1.5406 Å

Sample, annealing temperature [°C]	Phase composition		FWHM	Crystallite size, d_{xrd}, [nm]	Median particle size [μm]	Crystallinity, K [%]
	P1 [wt.%]	P2 [wt.%]				
$T_{0.2}$, 550	-	100	0.43	79	0.52	49
$T_{0.2}$, 800	9.0	91.0	0.39	87	0.49	54
$T_{0.5}$, 550	9.0	91.0	0.40	85	0.42	52
$T_{0.5}$, 800	20.7	79.3	0.37	91	0.44	52
T_1, 550	8.0	92.0	0.45	75	0.50	47
T_1, 800	48.5	51.5	0.54	63	0.48	48
T_3, 550	13.8	86.2	0.44	77	0.46	45
T_3, 800	21.6	78.4	0.40	85	0.47	51
T_5, 550	5.2	94.8	0.39	87	0.60	51

As seen from the data obtained, the use of different concentrations of ammonium hydroxide gives rather wide concentration range for hydrous zirconia synthesis resulting in the stepwise nature of hydrolysis and precipitation processes that remain independent of the chosen concentration. The increase in precipitator concentration results in the differences in precipitation rates. Latter leads to the observed changes in the structure of the gel and the properties of the resulting powders. Coupling the data on potentiometric titration, STA, SEM, BET and PSD, one can see that these changes occur consistently, demonstrating that ammonia is a suitable precipitant. While hydrolysis of zirconia is an inevitable process, the precipitation can be thoroughly controlled by ammonium hydroxide concentration. The increase in the concentration of ammonium hydroxide merely accelerates precipitation, the precipitator does not occlude in the gel and allows rather simple control of powder properties.

The use of the lowest concentration of ammonium hydroxide results in the finest size of particles (1.13±0.01 μm, Table 2), and the lowest temperature of phase transition from amorphous to crystalline zirconia (375±1 °C, Table 1 and Fig. 3), while the specific surface area of the $T_{0.2}$ sample remains lower than the value for the $T_{0.5}$ and T_1 powders. The dominant hydrolysis process results in the slight agglomeration of particles and the presence of the lamellar particles in the dendrite agglomerates (Fig. 4).

Annealing of the $T_{0.2}$ up to 800 °C results in the remarkable stability of the metastable tetragonal phase.

The use of 1 M ammonia solution for the reaction of hydrous zirconia formation results in the stoichiometric ratio of the reagents (Fig. 1). In case of more diluted and more concentrated ammonium hydroxide, the equivalence point is shifted due to the ageing of the gel and oxolation process. The obtained T_1 powder possesses the symmetric particle size distribution and rather large specific surface area. Synthesis by reverse co-precipitation with 1 M ammonia solution balances hydrolysis and precipitation processes, as a small amount of 0.1 M $ZrO(NO_3)_2$ solution is uniformly distributed in a sufficient amount of precipitant eliminating the need for excess of the reagents. Further calcination of the T_1 powder results in the tetragonal ZrO_2 with the admixture of monoclinic phase.

Comparison of the results obtained in the present work with the literature data [20,21,27,35] shows good data correlation between the crystallization temperature and precipitator concentration in zirconia powders. Indeed, similar increase of the crystallization temperature on the ammonia concentration was observed by Ushakov *et al.* [37] for yttria-stabilized zirconia ceramics. The increase of the ammonia content from 0.002 to 0.4 M resulted in the quasilinear increase in the crystallization temperature from 420 to 625 °C [37]. The obtained change was due to the nanoscaled particles effect. The use of ammonia provided the possibility to obtain nanoscaled particles of doped zirconia with the mean sizes lower than 100 nm. The specific surface area was also decreasing with the ammonia content increase. In the present work, the micron-scale agglomerated particles were obtained when 0.2 M ammonia solution was used to precipitate undoped zirconia. However, the observed stabilisation of the pure tetragonal phase can be also related to the stabilisation by the size-effect.

According to Keenan [27], the addition of dopants to zirconia stabilises the surface area of zirconia against sintering, i.e. generally increases the powder dispersity. The observed differences are also strongly related to the initial degree of hydration of zirconia, i.e. the structure of the precipitated hydrous zirconia [20]. These values differed significantly when zirconyl chloride and nitrate were used as initial salts for undoped zirconia precipitation [20,21,26], as well as when co-doped powders were synthesised [27,35]. Thus, the literature data on the effect of synthesis conditions on the dispersity, surface area and crystallization temperature should be analysed critically considering the dopant and zirconyl salt nature. In summary, in case of undoped zirconia synthesis the decrease of ammonia concentration to 0.2 M can be recommended as optimal to reach kinetic tetragonal phase stabilization. When it comes to doped zirconia powders, 1 M ammonia would be a preferable choice due to the better control of morphology and agglomeration of the resulting powders.

IV. Conclusions

The potentiometric titration revealed that the use of 1 M ammonia results in the stoichiometric reaction of zirconia precipitation. In case of 0.2, 0.5, 3 and 5 M ammonia precipitators the deviations from the reaction stoichiometry are due to the ageing of the gel and pronounced hydrolysis. By using DSC, it was shown that the temperature of the amorphous-to-crystal phase transition increases sharply by 77 °C when ammonia concentration increases from 0.2 to 0.5 M. By SEM and PSD analyses it was shown that the bimodal agglomerate distributions in the powders obtained using 0.2 M ammonia are due to the presence of lamellar particles in the dendrite agglomerates. Coupled results of BET, SEM and PSD showed that the specific surface area depends non-linearly on the ammonia content due to the varied nature of the agglomeration processes and lamellar particles present in the powders obtained in the diluted ammonia solution. It was shown by STA and XRD that the use of 0.2 M ammonia results in the kinetic stabilisation of pure tetragonal phase at 550 °C whereas small admixtures of monoclinic phase are present in the samples obtained using 0.5–5 M ammonia.

Acknowledgement: This work was supported by Russian science foundation (RSF #23-19-00236). BET measurements were performed at the Interdisciplinary Resource centre for innovative technologies for nanocomposite materials at the Research Park of St. Petersburg State University. STA measurements were performed at the Research Park of St. Petersburg State University Interdisciplinary Resource centre for thermogravimetric and calorimetric research. SEM measurements were performed at the Research Park of St. Petersburg State University Interdisciplinary Resource centre for nanotechnology.

References

1. J.R. Kelly, I. Denry, “Stabilized zirconia as a structural ceramic: An overview,” *Dental Mater.*, **24** [3] (2008) 289–298.
2. X. Zhang, X. Wu, J. Shi, “Additive manufacturing of zirconia ceramics: a state-of-the-art review”, *J. Mater. Res. Technol.*, **9** [4] (2020) 9029–9048.
3. J. Chevalier, “What future for zirconia as a biomaterial?”, *Biomaterials*, **27** [4] (2006) 535–543.
4. J. Chevalier, L. Gremillard, A.V. Virkar, D.R. Clarke, “The tetragonal-monoclinic transformation in zirconia: Lessons learned and future trends”, *J. Am. Ceram. Soc.*, **92** [9] (2009) 1901–1920.

5. F. Kern, H. Reveron, J. Chevalier, R. Gadow, "Mechanical behaviour of extremely tough TZP bioceramics", *J. Mech. Behav. Biomed. Mater*., **90** (2019) 395–403.
6. P. Khajavi, P.V. Hendriksen, H.L. Frandsen, "High-temperature degradation of tetragonal zirconia in solid oxide fuel and electrolysis cells: A critical challenge for long-term durability and a solution", *J. Eur. Ceram. Soc*., **44** [11] (2024) 6527–6539.
7. B. Charlas, H.L. Frandsen, K. Brodersen, P.V. Henriksen, M. Chen, "Residual stresses and strength of multilayer tape cast solid oxide fuel and electrolysis half-cells", *J. Power Sources*., **288** (2015) 243–252.
8. N. Mahato, A. Banerjee, A. Gupta, S. Omar, K. Balani, "Progress in material selection for solid oxide fuel cell technology: A review", *Prog. Mater. Sci*., **72** (2015) 141–337.
9. N. Izu, W. Shin, I. Matsubara, N. Murayama, N. Oh-hori, M. Itou, "Temperature independent resistive oxygen sensors using solid electrolyte zirconia as a new temperature compensating material", *Sens. Actuators B*, **108** [1-2] (2005) 216–222.
10. O.Yu. Kurapova, M.M. Pivovarov, K.V. Nikiforova, V.G. Konakov, "Sensor properties of stabilized zirconia ceramics, manufactured from nanopowders", *Rev. Adv. Mater. Sci.*, **57** [2] (2018) 257–261.
11. T. Liu, X. Zhang, L. Yuan, J. Yu, "A review of high-temperature electrochemical sensors based on stabilized zirconia", *Solid State Ionics*, **283** (2015) 91–102.
12. A. Pakseresht, F. Sharifianjazi, A. Esmaeilkhanian, L. Bazli, M. Reisi Nafchi, M. Bazli, K. Kirubaharan, "Failure mechanisms and structure tailoring of YSZ and new candidates for thermal barrier coatings: A systematic review", *Mater. Des*., **222** (2022) 111044.
13. R. Vaßen, M.O. Jarligo, T. Steinke, D.E. Mack, D. Stöver, "Overview on advanced thermal barrier coatings", *Surf. Coat. Technol*., **205** [4] (2010) 938–942.
14. E. Roitero, H. Reveron, L. Gremillard, V. Garnier, C. Ritzberger, J. Chevalier, "Ultra-fine yttria-stabilized zirconia for dental applications: A step forward in the quest towards strong, translucent and aging resistant dental restorations", *J. Eur. Ceram. Soc*., **43** [7] (2023) 2852–2863.
15. P. Khajavi, H.L. Frandsen, L. Gremillard, J. Chevalier, P.V. Hendriksen, "Strength and hydrothermal stability of NiO–stabilized zirconia solid oxide cells fuel electrode supports", *J. Eur. Ceram. Soc*., **41** [7] (2021) 4206–4216.
16. J. Chevalier, J. Loh, L. Gremillard, S. Meille, E. Adolfson, "Low-temperature degradation in zirconia with a porous surface", *Acta Biomater*., **7** [7] (2011) 2986–2993.
17. R.C. Garvie, "The occurrence of metastable tetragonal zirconia as a crystallite size effect", *J. Phys. Chem*., **69** [4] (1965) 1238–1243.
18. H. Reveron, M. Fornabaio, P. Palmero, T. Fürderer, E. Adolfsson, V. Lughi, A. Bonifacio, V. Sergo, L. Montanaro, J. Chevalier, "Towards long lasting zirconia-based composites for dental implants: Transformation induced plasticity and its consequence on ceramic reliability", *Acta Biomater*., **48** (2017) 423–432.
19. S. Shukla, S. Seal, R. Vanfleet , "Sol-gel synthesis and phase evolution behavior of sterically stabilized nanocrystalline zirconia", *J. Sol-Gel Sci. Technol*., **27** [2] (2003) 119–136.
20. G.A. Carter, R.D. Hart, M.R. Rowles, C.E. Buckley, M.I. Ogden, "The effect of processing parameters on particle size in ammonia-induced precipitation of zirconyl chloride under industrially relevant conditions", *Powder Technol*., **191** [1-2] (2009) 218–226.
21. G.A. Carter, M. Rowles, M.I. Ogden, R.D. Hart, C.E. Buckley, "Industrial precipitation of zirconyl chloride: The effect of pH and solution concentration on calcination of zirconia", *Mater. Chem. Phys*., **116** [2-3] (2009) 607–614.
22. R. Stevens, *Introduction to Zirconia*, Magnesium Elektron, Swinton Manchester, 1986.
23. O.Yu. Kurapova, V.G. Konakov, "Phase evolution in zirconia based systems", *Rev. Adv. Mater. Sci*., **36** [2] (2014) 177–190.
24. N.N. Novik, V.G. Konakov, I.Y. Archakov, "Zirconia and ceria based ceramics and nanoceramics - A review on electrochemical and mechanical properties", *Rev. Adv. Mater. Sci*., **40** [2] (2015) 188–207.
25. E. Ivanova, V. Konakov, E. Solovieva, "The synthesis of nano-sized powders in the ZrO_2-HfO_2-Y_2O_3 system", *Rev. Adv. Mater. Sci.*, **4** [1] (2003) 41–47.
26. T.E. Lomakina, Y.V. Konakov, I.Yu. Archakov, O.Yu. Kurapova, V.G. Konakov, "The effect on zirconyl type salt on the phase composition, particle size and sinterability of zirconia based powders obtained via reversed co-precipitation", *J. Sol-Gel Sci. Technol*., **113** [3] (2025) 926–941.
27. M. Keenan, "The influence of dopants on the surface properties of zirconia", *Ph.D. thesis*, The Nottingham Trent University, 1997.
28. Z. Huang, W. Han, Z. Feng, J. Qi, D. Wu, N. Wei, Z. Tang, Y. Zhang, J. Duan, T. Lu, "The effects of precipitants on co-precipitation synthesis of yttria-stabilised zirconia nanocrystalline powders", *J. Sol-Gel Sci. Technol*., **90** [2] (2019) 359–368.
29. B. Vörös-Horváth, A. Salem, B. Kovács, A. Széchenyi, S. Pál, "Systematic study of reaction conditions for size-controlled synthesis of silica nanoparticles", *Nanomaterials*., **14** [19] (2024) 1561.
30. C.A. Cortés Escobedo, J. Muñoz-Saldaña, D. Jaramillo-Vigueras, F.J. Espinoza-Beltrán, "Preparation of size controlled nanometric spheres of colloidal silica for synthetic opal manufacture", *Mater. Sci. Forum*., **509** (2006) 187–192.
31. H.-J. Noh, D.-S. Seo, H. Kim, J.-K. Lee, "Synthesis and crystallization of anisotropic shaped ZrO_2 nanocrystalline powders by hydrothermal process", *Mater. Lett*., **57** [16-17] (2003) 2425–2431.
32. O.Yu. Kurapova, S.N. Golubev, V.M. Ushakov, V.G. Konakov, "Stabilization of cubic zirconia based solid solutions obtained by cryochemical techniques: Thermodynamic and kinetic factors", *Rev. Adv. Mater. Sci.*, **48** [2] (2017) 147–155.
33. D. Qi, C. Lin, H. Zhao, H. Liu, T. Lü, "Size regulation and prediction of the SiO_2 nanoparticles prepared via Stöber process", *J. Dispers. Sci. Technol*., **38** [1] (2017) 70–74.
34. H.J. Cha, O.K. Park, Y.H. Kim, H.G. Cha, Y.S. Kang, "Tretmant of TiO_2 for the suppression of photo-catalytic property and dispersion stability", *Int. J. Nanosci*., **5** [6] (2006) 795–801.

35. Y. Suyama, T. Mizobe, A. Kato, "ZrO_2 powders produced by vapor phase reaction", *Ceram. Int.*, **3** [4] (1977) 141–146.
36. V. Konakov, S. Seal, E. Solovieva, M. Pivovarov, A. Shorochov, "Influence of precursor dispersity and agglomeration of mechanical characteristics of $92ZrO_2$-$8Y_2O_3$ ceramics", *Rev. Adv. Mater. Sci.*, **13** [1] (2006) 71–76.
37. S.V. Ushakov, C.E. Brown, A. Navrotsky, A. Demkov, C. Wang, B.-Y. Nguyen, "Thermal analyses of bulk amorphous oxides and silicates of zirconium and hafnium", *MRS Proceedings*, **745** (2002) 14.
38. O.Yu. Kurapova, D.V. Nechaeva, A.V. Ivanov, S.N. Golubev, V.M. Ushakov, V.G. Konakov, "Thermal evolution of the microstructure of calcia stabilized zirconia precursors manufactured by cryochemical technique", *Rev. Adv. Mater. Sci.*, **47** [1-2] (2016) 95–104.
39. J. Rouquerol, F. Rouquerol, P. Llewellyn, G. Maurin, K. Sing, *Adsorption by Powders and Porous Solids: Principles, Methodology and Applications*, Academic Press, 2013.
40. C. Brinker, G. Scherer, *Sol-Gel Science: The Physics and Chemistry of Sol-Gel Processing*, Gulf Professional Publishing, 1990.